Coupling Self-Attention Generative Adversarial Network and Bayesian Inversion for Carbon Storage System

Jichao Bao [1] **Jonghyun Lee** [1] **Hongkyu Yoon** [2]

Abstract

Characterization of geologic heterogeneity at a geological carbon storage (GCS) system is crucial for cost-effective carbon injection planning and reliable carbon storage. With recent advances in computational power and sensor technology, large-scale fine-resolution simulations of multiphase flow and reactive transport processes have been available. However, traditional large-scale inversion approaches have limited utility for sites with complex subsurface structures such as faults and microfractures within the host rock matrix. In this work, we present a Bayesian inversion method with deep generative priors tailored for the computationally efficient and accurate characterization of GCS sites. Self-attention generative adversarial network (SAGAN) is used to learn the approximate subsurface property (e.g., permeability and porosity) distribution from discrete fracture network models as a prior and accelerated stochastic inversion is performed on the low-dimensional latent space in a Bayesian framework. Numerical examples with a synthetic fracture field with pressure and heat tracer data sets are presented to test the accuracy, speed, and uncertainty quantification capability of our proposed joint data inversion method.

1. Introduction

For the subsurface inverse problem (Carrera et al., 2005; McLaughlin & Townley, 1996; Oliver et al., 2008), spatially distributed geologic parameters such as permeability and porosity are estimated from noisy and sparse hydrogeophysical and geomechanical measurements such as pressure, temperature, displacement, seismic responses, and so on. Due to ill-posedness in the inverse problem, probabilistic frameworks have been implemented in order to account for the uncertainty that provides both unknown subsurface parameters and their corresponding uncertainty in a Bayesian statistical framework (e.g., Kitanidis, 1995; 2010; Lee et al., 2016). Typically pressure measurements from injection-extraction well operations are used for the site characterization, but unless many injection/extraction/observation wells are available, the subsurface characterization with sparse pressure measurements leads to poor predictions of other relevant quantities such as reactive transport. To overcome this issue, different sensing data can be used for joint inversion of pressure, saturation, temperature, and seismicity to identify the subsurface geologic connectivity during the CO_2 sequestration operations (Chen et al., 2018).

Still, one of the challenges in subsurface characterization is to identify highly heterogeneous permeability fields such as reservoirs with fracture networks. For such cases, traditional techniques using the Gaussian prior lead to smoothed, low-resolution images of subsurface properties with high estimation uncertainty due to the diffusive nature of the governing equations. Machine learning techniques such as deep generative models (Kang et al., 2022; 2021; Yoon et al., 2022; Kadeethum et al., 2021) have been actively studied to enforce the subsurface solution space on the relevant prior distribution constructed through multipoint geostatistics-based training images.

In this work, we present an application of an inverse modeling method based on the self-attention generative adversarial network (SAGAN) (Zhang et al., 2019) for characterizing a subsurface reservoir field at a reduced computational cost with improved accuracy compared to traditional inversion. The multiphysics model MOOSE-FALCON (Podgorney et al., 2021) is combined with our proposed Bayesian latent space inversion method. A synthetic application with single-phase flow pressure and heat tracer data is considered in this work for a two-dimensional, strongly heterogeneous permeability field estimation. Inversion of synthetic injecting tests is performed to show the usefulness and practicality of the proposed approach for geological carbon storage (GCS) sites characterization with reasonable accuracy before the

[1]University of Hawaii at Manoa, Honolulu, HI, USA [2]Sandia National Laboratories, Albuquerque, NM, USA. Correspondence to: Jonghyun Lee <jonghyun.harry.lee@hawaii.edu>.

Accepted after peer-review at the 1st workshop on Synergy of Scientific and Machine Learning Modeling, SynS & ML ICML, Honolulu, Hawaii, USA. July, 2023.

proposed method is extended and applied to 3D GCS applications.

2. Method

2.1. Deep Generative Modeling

Deep generative models (Goodfellow et al., 2014) have been studied because of their capability to approximate data distributions from training samples and generate new samples from the approximated data distribution in an efficient fashion. We use the self-attention generative adversarial network (SAGAN), which applies self-attention mechanism and spectral normalization (Zhang et al., 2019). SAGAN creates samples with detailed features from low-dimensional latent variables, which provides a solution for learning the distribution of subsurface properties such as fracture networks. 50,000 images with randomly generated fractures were used for training. There are 30 fractures at $0°$, 30 fractures at $90°$, and 40 fractures at $135°$ in each image, and the length of the fractures ranges from 5 to 20 pixels, similar to the images shown in Figure 3. The inversion solutions are constrained to the learned latent space while consistent with the observations. This will lead to our deep generative model-based parameterization of the permeability field:

$$\mathbf{s} = G(\mathbf{z}) \tag{1}$$

where $\mathbf{s}$ is the permeability field and $\mathbf{z}$ is a k ($\ll m$)-dimensional (m represents the dimension of the permeability field) latent variable constructed from SAGAN. Using our generator $G(\mathbf{z})$, the variable $\mathbf{z}$ in the context of the inversion problem represents the low-dimensional representation of $\mathbf{s}$.

2.2. Bayesian Inversion using Deep Generative Modeling

We use a Hierarchical Bayesian approach combined with SAGAN in this work for the inverse problem solver. The forward problem with the input of permeability field $\mathbf{s}$ can be defined in the form of the relationship

$$\mathbf{y} = \mathbf{h}(\mathbf{s}) + \boldsymbol{\varepsilon} \tag{2}$$

where $\mathbf{y}$ is the observation (*e.g.*, pressure, saturation, temperature, and displacement), $\boldsymbol{\varepsilon}$ is the observation and model uncertainty noise such as a Gaussian distribution with mean zero $\boldsymbol{\varepsilon} \sim \mathcal{N}(\mathbf{0}, \mathbf{R})$. Here, $\mathbf{R}$ is the model/observation error matrix and $\mathbf{h}$ is the forward map. The inverse problem equivalent of Eq. 2 can be defined as a problem with unknown m-dimensional variable $\mathbf{s}$ (permeability) and n (noisy) observation $\mathbf{y}$ (pressure, temperature, and displacement). The Bayes' rule allows us to evaluate a posterior distribution of $\mathbf{s}$ via

$$p(\mathbf{s}|\mathbf{y}) \propto p(\mathbf{y}|\mathbf{s})p'(\mathbf{s}) = \int_{\boldsymbol{\theta}} p(\mathbf{y}|\mathbf{s})p'(\mathbf{s}|\boldsymbol{\theta})p'(\boldsymbol{\theta})d\boldsymbol{\theta} \tag{3}$$

where $p'(\cdot)$ represents the prior probability and $\boldsymbol{\theta}$ is a set of hyperparameters that models $\mathbf{s}$ in a hierarchical Bayesian framework.

In particular, with the generator G, we can constrain variable $\mathbf{z}$ to follow a Gaussian distribution to ensure the regularity of the latent space:

$$\mathbf{z} \sim \mathcal{N}(\mathbf{0}, \boldsymbol{\Sigma}) \tag{4}$$

We also assume that G is a deterministic map from $\mathbf{z}$ to $\mathbf{s}$ and the hyperparameter $p'(\boldsymbol{\theta})$ such as neural network model parameters follows a delta distribution:

$$\boldsymbol{\theta} = \boldsymbol{\delta}(\boldsymbol{\theta} - \hat{\boldsymbol{\theta}}) \tag{5}$$

This allows us to rewrite Eq. 3 in the form

$$\begin{aligned} p(\mathbf{z}|\mathbf{y}) &\propto p(\mathbf{y}|\mathbf{z})p'(\mathbf{z}) \\ &\propto \exp\left(-(\mathbf{y} - \mathbf{h}(G(\mathbf{z})))^\top \mathbf{R}^{-1}(\mathbf{y} - \mathbf{h}(G(\mathbf{z})))\right) \\ &\quad \cdot \exp\left(-\mathbf{z}^\top \boldsymbol{\Sigma}^{-1}\mathbf{z}\right) \end{aligned} \tag{6}$$

We explore this posterior equation to identify the latent variables consistent with observations through sampling or Bayesian approaches. Here we use a Bayesian approach to find the maximum a posteriori (MAP) estimate, which is the mode of the posterior distribution.

This task will require the computation of Jacobian $\mathbf{J}^l$ and at the lth iteration the computation is given by

$$\begin{aligned} \mathbf{J}^l = \left.\frac{\partial \mathbf{h}(G(\mathbf{z}))}{\partial \mathbf{z}}\right|_{\mathbf{z}=\mathbf{z}^l} &= \left.\frac{\partial \mathbf{h}}{\partial \mathbf{s}}\right|_{\mathbf{s}=G(\mathbf{z}^l)} \left.\frac{\partial \mathbf{s}}{\partial \mathbf{z}}\right|_{\mathbf{z}=\mathbf{z}^l} \\ &= \left.\mathbf{J}_\mathbf{h}\right|_{\mathbf{s}=G(\mathbf{z}^l)} \left.\mathbf{J}_G\right|_{\mathbf{z}=\mathbf{z}^l} \end{aligned} \tag{7}$$

Note that $\frac{\partial \mathbf{s}}{\partial \mathbf{z}}$ can be evaluated analytically using automatic differentiation (AD). This information can be provided at no additional computational cost in common libraries such as TensorFlow and PyTorch. Since the dimension of $\mathbf{z}$ is assumed to be significantly smaller than the dimension of $\mathbf{s}$, e.g., $dim(z) \leq 100$, we can also use a finite difference formulation to calculate the Jacobian matrix as an alternative to AD.

The workflow of coupling SAGAN and Bayesian inversion is shown in Figure 1. Using the trained generator, the 128×128 permeability field is generated with 16 latent variables. FALCON is then used as a forward model h in Eq. 2 and latent variables are updated using Bayesian inversion to maximize the negative logarithm of Eq. 6

3. Synthetic Example Setup

The domain for heterogeneity characterization is a synthetic two-dimensional depth-integrated deep formation. As

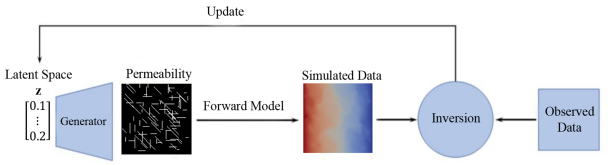

Figure 1. The workflow of coupling SAGAN and Bayesian inversion

shown in Figure 2, a 640 m $\times$ 640 m domain was discretized into 128 $\times$ 128 meshes. This image shows fractures with 3 orientations: $0°$, $90°$, and $135°$, and this image was not used for training. A constant pressure of 34 MPa and 30 MPa was imposed on the western and eastern boundaries, respectively. A constant temperature of 473.15 K and 423.15 K was applied to the western and eastern boundaries, respectively. One injection well was placed at [190 m, 180 m] for transient simulations and nine monitoring wells were used for observation. To simplify the problem formulation, we inject heat tracer (lower temperature water than one in the deep formation) into the aquifer, and pressure and temperature data were measured every 100 s at the monitoring wells. The injection rates linearly increased from 0 to 5 g/s from 0 s to 1000 s. The injection temperature was a constant value of 323.15 K. The values of the material parameters are shown in Table 1. Permeability and porosity are heterogeneous as shown in Figure 3, using the same image but assigning different values. For permeability, the fractures (white lines) were assigned 10^{-14} m^2, and other areas were assigned 10^{-16} m^2. For porosity, the fractures were assigned 10^{-3}, and other areas were assigned 10^{-4}.

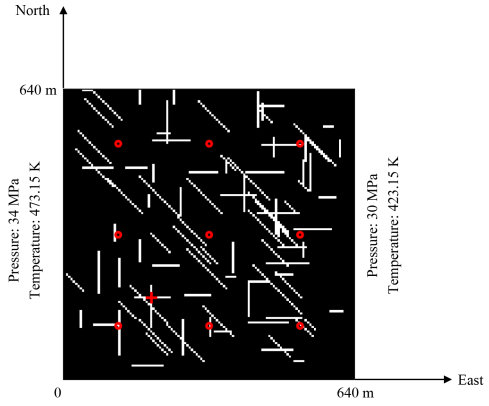

Figure 2. Model settings. 34 MPa pressure and 473.15 K temperature were applied to the western boundary. 30 MPa pressure and 423.15 K temperature were applied to the eastern boundary. The red circles represent monitoring wells, and the red cross shows the injection well location.

Table 1. Material parameters.

Parameter	Unit	Value
Permeability	m^2	heterogeneous
Porosity	–	heterogeneous
Density	kg/m^3	2640
Specific heat	$J/kg \cdot K$	790
Thermal conductivity	$W/m \cdot K$	3.05

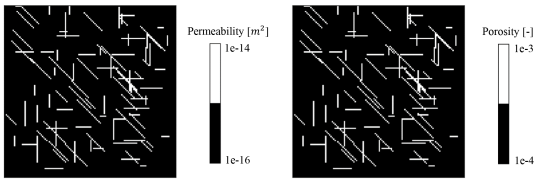

Figure 3. Permeability and porosity

4. Preliminary Results

Figure 4 shows the estimation of the permeability field which shows reasonable characterization of subsurface fracture features because of the informative training data for the deep generative model construction. Figure 5 shows the fitting results of pressure and temperature data. Gaussian noise with standard deviations of 1% of the mean was added to the observed pressure and temperature data, respectively. The fitting errors are also shown as the root mean square error (RMSE):

$$RMSE = \sqrt{\frac{1}{N_k}\sum_{i=1}^{N_k}(\mathbf{k}_i^{est} - \mathbf{k}_i^{true})^2} \tag{8}$$

where $\mathbf{k}_i^{est}$ indicates the estimated parameter value and $\mathbf{k}_i^{true}$ is the true value, N_k is the total number of parameters.

The RMSE of pressure data fitting is 0.351 while the RMSE of temperature data fitting is 4.266, about the same level as the error added. We estimated permeability and porosity together and the accuracy of the porosity estimate is similar to the permeability estimation.

5. Conclusion

We implemented a deep generative model-based inversion approach to perform joint data inversions and presented reasonable inversion results with affordable forward model runs. The proposed method transforms an inverse problem with the computational cost associated with the number of observations into an approximately same problem with a constant number ($\sim$total O(100)) of simulations so that one would expect a great computational gain in solving high-dimensional inverse problems. In the examples presented,

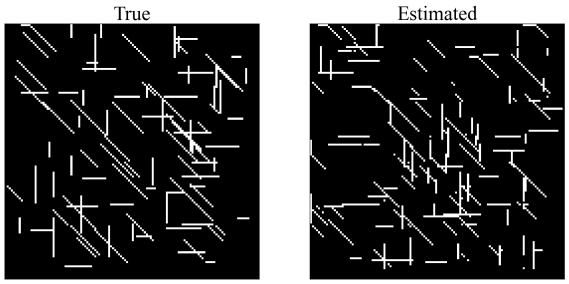

Figure 4. Estimation result; the true permeability field is shown on the left and the estimated field is shown on the right.

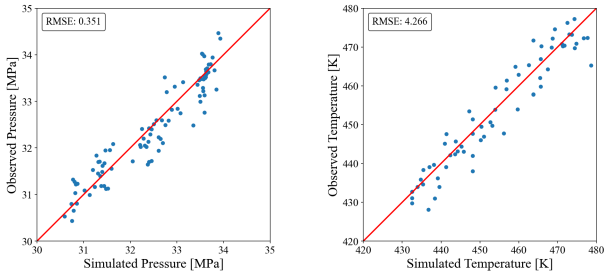

Figure 5. Pressure and temperature data fitting. Fitting errors are shown in RMSE. The measurement locations are indicated by the red circles in Figure 2 with an interval of 200 m.

the estimated fields captured important permeability features, i.e., fractures, due to the informative prior used in the training. It is also observed that the estimate with improved accuracy was obtained at a much smaller computational cost than traditional methods, allowing for the characterization of a 2D deep reservoir in less than 10 minutes on a workstation equipped with 48 CPU cores. Joint data inversion from pressure and heat tracer with the pre-trained deep generative model can be beneficial to identify connectivity features in the site without considerably increasing the computational costs.

6. Broader Impact

Understanding the distribution of subsurface properties such as permeability and porosity is important for CO_2 storage management. Our work aims to develop an efficient and fast inverse modeling framework to estimate key parameters of subsurface storage sites, then better predict flow and transport processes. Well placement and CO_2 injection planning will benefit from characterization of subsurface properties and predictions.

Acknowledgments

This work was supported by US Department of Energy Office of Fossil Energy and Carbon Management, the Science-informed Machine Learning for Accelerating Real-Time Decisions in Subsurface Applications (SMART) Initiative.

Sandia National Laboratories is a multi-mission laboratory managed and operated by National Technology & Engineering Solutions of Sandia, LLC (NTESS), a wholly owned subsidiary of Honeywell International Inc., for the U.S. Department of Energy's National Nuclear Security Administration (DOE/NNSA) under contract DE-NA0003525. This written work is authored by an employee of NTESS. The employee, not NTESS, owns the right, title and interest in and to the written work and is responsible for its contents. Any subjective views or opinions that might be expressed in the written work do not necessarily represent the views of the U.S. Government. The publisher acknowledges that the U.S. Government retains a non-exclusive, paid-up, irrevocable, world-wide license to publish or reproduce the published form of this written work or allow others to do so, for U.S. Government purposes. The DOE will provide public access to results of federally sponsored research in accordance with the DOE Public Access Plan.

References

Carrera, J., Alcolea, A., Medina, A., Hidalgo, J., and Slooten, L. J. Inverse problem in hydrogeology. *Hydrogeology Journal*, 13(1):206–222, 2005.

Chen, B., Harp, D. R., Lin, Y., Keating, E. H., and Pawar, R. J. Geologic co2 sequestration monitoring design: A machine learning and uncertainty quantification based approach. *Applied energy*, 225:332–345, 2018.

Goodfellow, I., Pouget-Abadie, J., Mirza, M., Xu, B., Warde-Farley, D., Ozair, S., Courville, A., and Bengio, Y. Generative adversarial nets. In *Advances in neural information processing systems*, pp. 2672–2680, 2014.

Kadeethum, T., O'Malley, D., Fuhg, J. N., Choi, Y., Lee, J., Viswanathan, H. S., and Bouklas, N. A framework for data-driven solution and parameter estimation of pdes using conditional generative adversarial networks. *Nature Computational Science*, 1(12):819–829, 2021.

Kang, X., Kokkinaki, A., Kitanidis, P. K., Shi, X., Lee, J., Mo, S., and Wu, J. Hydrogeophysical characterization of nonstationary dnapl source zones by integrating a convolutional variational autoencoder and ensemble smoother. *Water Resources Research*, 57(2): e2020WR028538, 2021.

Kang, X., Kokkinaki, A., Shi, X., Yoon, H., Lee, J., Kitanidis, P. K., and Wu, J. Integration of deep learning-based inversion and upscaled mass-transfer model for dnapl mass-discharge estimation and uncertainty assessment. *Water Resources Research*, 58(10):e2022WR033277, 2022.

Kitanidis, P. K. Quasi-linear geostatistical theory for inversing. *Water Resources Research*, 31(10):2411–2419, 1995. ISSN 0043-1397.

Kitanidis, P. K. *Bayesian and Geostatistical Approaches to Inverse Problems*, pp. 71–85. John Wiley & Sons, Ltd, 2010.

Lee, J., Yoon, H., Kitandis, P. K., Werth, C. J., and Valocchi, A. J. Scalable subsurface inverse modeling for a big data set with an application to massive magnetic resonance imaging tracer concentration data inversion. *Water Resources Research*, 52(7):5213–5231, 2016.

McLaughlin, D. and Townley, L. R. A reassessment of the groundwater inverse problem. *Water Resources Research*, 32(5):1131–1161, 1996.

Oliver, D. S., Reynolds, A. C., and Liu, N. *Inverse theory for petroleum reservoir characterization and history matching*. Cambridge University Press, Cambridge ; New York, 2008.

Podgorney, R., Finnila, A., Simmons, S., and McLennan, J. A reference thermal-hydrologic-mechanical native state model of the utah forge enhanced geothermal site. *Energies*, 14(16):4758, 2021.

Yoon, H., Lee, J., and Kadeethum, T. Deep learning-based data assimilation in the latent space for real-time forecasting of geologic carbon storage. *Available at SSRN 4294901*, 2022. doi: Doi10.2139/ssrn.4294901.

Zhang, H., Goodfellow, I., Metaxas, D., and Odena, A. Self-attention generative adversarial networks. In *International conference on machine learning*, pp. 7354–7363. PMLR, 2019.